

# Magnetic field dependence of valley splitting in realistic Si/SiGe quantum wells

Mark Friesen, M. A. Eriksson, and S. N. Coppersmith  
*Department of Physics, University of Wisconsin, Madison, WI 53706*

The authors investigate the magnetic field dependence of the energy splitting between low-lying valley states for electrons in a Si/SiGe quantum well tilted with respect to the crystallographic axis. The presence of atomic steps at the quantum well interface may explain the unexpected, strong suppression of the valley splitting observed in recent experiments. The authors find that the suppression is caused by an interference effect associated with multiple steps, and that the magnetic field dependence arises from the lateral confinement of the electronic wave function. Using numerical simulations, the authors clarify the role of step disorder, obtaining quantitative agreement with the experiments.

Qubits in silicon are leading candidates for scalable quantum computing, owing to their favorable and well studied materials properties.<sup>1,2</sup> Indeed, because of its prominence in the electronics industry, silicon may be the best understood semiconducting material. However, as devices continue to shrink in size, approaching the quantum regime, important questions arise. Unlike direct gap semiconductors, the conduction band structure in silicon possesses six symmetric minima or “valleys” that are not at the Brillouin zone center. Consequently, the minima are degenerate, and must be described by a valley index which competes with the spin index as a relevant quantum number in the qubit Hilbert space.<sup>3</sup> Therefore, to construct spin qubits in silicon, it is necessary to lift all valley degeneracy.

A silicon quantum well grown on the [001] surface of strain-relaxed silicon-germanium is under tensile strain, causing the four lateral valleys to rise significantly in energy.<sup>4</sup> At low temperatures, only the two low-lying valleys are populated. The remaining two-fold degeneracy can be removed by the sharp confinement potential of the quantum well interface.<sup>5</sup> Theoretical estimates suggest that the resulting valley splitting can be of the order of 1 meV  $\approx$  12 K,<sup>6</sup> which is sufficiently large for quantum computing. However, recent experiments in SiGe<sup>7,8,9,10</sup> measure a valley splitting much smaller than the theoretical prediction. There is currently no explanation for this discrepancy.<sup>11</sup> Indeed, a prevalent theory<sup>12</sup> predicts an enhancement of the valley splitting in a magnetic field that is different from the experimental observations.

In this letter, we describe a single-electron valley splitting theory for silicon quantum wells grown on a vicinal substrate, building upon an initial suggestion by Ando.<sup>13</sup> Such miscuts are often incorporated into Si/SiGe heterostructures to ensure uniform growth surfaces and to avoid step bunching. The resulting quantum well, obtained by conformal epitaxial deposition, is misaligned with respect to the crystallographic  $z$  axis, as shown in Fig. 1. We now describe the effective mass theory and explain how the presence of interfacial atomic steps suppresses valley splitting.

For silicon strained in the [001] direction, the effective mass wavefunction<sup>14</sup> can be written as a sum of contri-

butions from the two  $z$  valleys:<sup>15</sup>

$$\Psi(\mathbf{r}) = \frac{1}{\sqrt{2}} [e^{ik_0 z} u_{k_0}(\mathbf{r}) + e^{-ik_0 z + i\phi} u_{-k_0}(\mathbf{r})] F(\mathbf{r}). \quad (1)$$

where the terms inside brackets are Bloch functions. The phase angle  $\phi$  is determined by the position of the quantum well interface.<sup>15</sup> The two orthogonal valley states correspond to a phase difference of  $\Delta\phi = \pi$ , although the absolute value of  $\phi$  is unimportant in the present discussion. It is crucial to note that while the valley minima occur along the  $z$  axis at  $\pm k_0 \hat{z}$ , the quantum well normal is tilted away from  $\hat{z}$ . For a slowly varying confinement potential, the two valleys have the same envelope function, and are essentially independent. However, sharp variations in the potential cause the effective mass approximation to break down. Examples include the central cell potential near a shallow donor,<sup>16</sup> and the sharp band offsets at the interface of a quantum well.<sup>15</sup> Leading order corrections to the effective mass theory<sup>15</sup> give the valley splitting

$$E_v = 2 \left| \int d\mathbf{r}^3 e^{-i2k_0 z} |F(\mathbf{r})|^2 V_v(\mathbf{r}) \right|, \quad (2)$$

where the coupling potential  $V_v(\mathbf{r})$  decays a few Angströms from the interface. Because this decay length is so small, compared to effective mass length scales, it can be represented as a  $\delta$  function:

$$V_v(\mathbf{r}) = v_v \delta(z - z_i), \quad (3)$$

where  $z_i(x)$  is the position of the interface along the  $x$  axis. The coupling parameter  $v_v$  contains atomic scale information that must be obtained from *ab initio* theories such as tight-binding theory,<sup>15</sup> or from experiments. The phase factor in Eq. (2) reflects the valley separation of  $2k_0$ , and plays a crucial role in the theory by introducing interference effects, as we shall see. Note that large modulation doping fields usually confine the wave function to one side of the quantum well, so only one interface potential has been included in Eq. (3).

We can now explain the suppression of the valley splitting. In a tilted quantum well, the interface position  $z_i(x)$  describes the atomic steps, as shown in Fig. 1. The  $\delta$  function in Eq. (3) reduces the  $E_v$  integral to a sum over

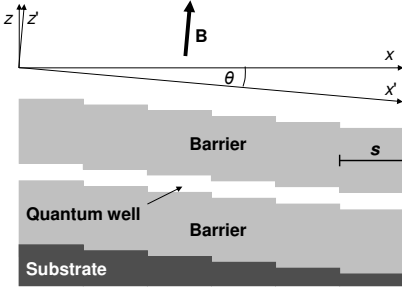


FIG. 1: Quantum well step geometry, with crystallographic axes  $(x, y, z)$  and rotated axes  $(x', y', z')$ , where  $y = y'$ .

steps with phase angles differing by  $2k_0b \simeq 0.85\pi$ . Here,  $k_0 \simeq 0.85(\pi/2b)$ , and  $b \simeq 1.358 \text{ \AA}$  is the atomic step height. Thus, the phases from consecutive steps interfere almost fully destructively. For a delocalized electron, the wavefunction extends over an infinite number of steps, resulting in the complete suppression of  $E_v$ . In the presence of a magnetic field, the electronic wave function is confined to a finite number of steps, leading to a non-vanishing valley splitting.

We can estimate the valley splitting at low magnetic fields from Eq. (2), assuming the idealized (but unrealistic) miscut geometry shown in Fig. 1, with uniform steps of equal width. A high-field tight-binding theory was presented in Ref. 17 for the same geometry. A good approximation for the wave function of an electron in a perpendicular magnetic field and a tilted quantum well is given by the well-known solution for a flat quantum well,<sup>18</sup> in the rotated basis  $(x', y', z')$  shown in Fig. 1. For the lowest ( $n = 0$ ) eigenstate corresponding to the symmetric gauge,  $\mathbf{A} = (-y', x', 0)B/2$ , we obtain<sup>18</sup>  $F(\mathbf{r}') = F_{xy}(x', y')F_z(z')$ , where  $F_{xy}(x', y') = e^{-(x'^2+y'^2)/4l_B^2}/\sqrt{2\pi l_B^2}$  and  $F_z(z')$  is the subband envelope. Here, the electronic wave function is confined over the magnetic length scale  $l_B = \sqrt{\hbar/|eB|}$ . For large  $l_B$ , we can ignore the discreteness of the atomic steps in  $z_i(x)$ . Performing the integral in Eq. (2), we obtain  $E_v \simeq 2v_v F_z^2(0)e^{-2(k_0 l_B \theta)^2}$ , where  $\theta \ll 2\pi$  is the miscut angle. Thus, for uniform steps, the valley splitting is suppressed exponentially in  $B$ , as confirmed by the numerical analysis described below.

The previous results are strongly affected by even a little disorder. At low fields, disorder can enhance the valley splitting by many orders of magnitude, showing that the exponential suppression occurs because of a delicate cancellation of the phase terms in Eq. (2). To investigate the effects of disorder, we have performed numerical simulations of the valley splitting. We introduce adjustable parameters describing the amplitude of normally-distributed fluctuations, or wiggles, of the step edges. The fluctuation model incorporates alternating smooth and rough step edges, as consistent with the experimental data.<sup>19</sup> Typically in our simulations, the amplitude of the rough step fluctuations is set at its charac-

teristic “large” value  $s$ , corresponding to the average step separation. We also introduce a step-bunching parameter, which allows neighboring step edges to overlap. Such bunching is known to occur at silicon growth interfaces, particularly under the influence of strain.<sup>20</sup> A representative step profile is shown in Fig. 2(a). To make contact with the data of Ref. 10, we consider a  $2^\circ$  miscut.

For a given, randomly generated step profile, we evaluate Eq. (2) numerically. The resulting valley splitting now depends on the electron position, since disorder breaks the translational symmetry. In the symmetric gauge, the unperturbed magnetic wave function can be centered, degenerately, at different points in space. By computing the valley splitting for wave functions centered at each of these points, we obtain a valley splitting landscape,  $E_v(\mathbf{r}')$ , including peaks and valleys. Electrons are attracted to the valley splitting peaks in order to minimize their total energy. We observe that peaks always occur near broad step fluctuations, or “plateaus,” and that bunched steps tend to produce the strongest valley splitting peaks. By tracking the dominant peak in a given cell, we can determine  $E_v(B)$  for a fixed step profile. In Eq. (3) we use  $v_v \simeq 1.2 \times 10^{-11} \text{ eV} \cdot \text{m}$ , as obtained in Ref. 15, which corresponds to a  $\text{Si}_{0.7}\text{Ge}_{0.3}/\text{Si}/\text{Si}_{0.7}\text{Ge}_{0.3}$  quantum well.

Some typical simulation results for  $E_v(B)$  are shown in Fig. 2(b). By setting the step fluctuations to their characteristic “large” value, as described above, we obtain reasonable agreement with the experimental data of Ref. 10 for any value of the step bunching parameter. By fine tuning the step-bunching parameter, we obtain the best quantitative agreement when the average bunching length is in the range of 10-20s.

In the intermediate field range  $0.3 < B < 3 \text{ T}$ , the experimental data points in Fig. 2 are strikingly linear.<sup>10</sup> The corresponding simulation results exhibit a slightly sublinear field dependence. More generally, we find that the precise shape of the  $E_v(B)$  curves depends on the particular disorder realization and the fluctuation model. It is very likely that other disorder models, not considered here, could produce different curve shapes, including the linear behavior of the data. One idealized model giving a linear valley splitting is the “plateau” model, corresponding to wide, localized, flat plateaus surrounded by relatively uniform steps. The valley splitting contribution from the ordered steps surrounding the plateau is strongly suppressed, due to the cancellation effects described above, so that the plateaus dominate the valley splitting. The scaling theory for an isolated plateau is obtained by introducing the concept of an “excess area”  $A$  relative to a perfectly uniform step configuration. For a small magnetic field, the electronic wave function is spread out over the large area  $2\pi l_B^2$ . The resulting valley splitting in this model is

$$E_v \simeq v_v F_z^2(0)A/\pi l_B^2, \quad (4)$$

which is linear in  $B$ . We can obtain an experimental estimate for  $A$  from the data of Ref. 10. Using theoretical

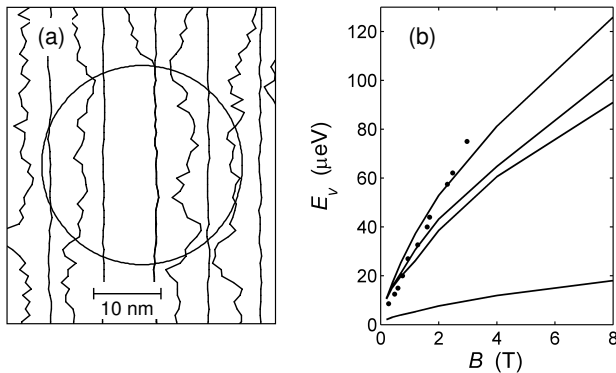


FIG. 2: Realistic valley splitting simulations. (a) A randomly generated step edge profile, with alternating smooth and rough step edges. The circle shows the wave function radius  $l_B$  for  $B = 3$  T, centered at the position of the valley splitting maximum. (b) Simulation results for the valley splitting (solid lines). Experimental data points (circles) are taken from Ref. 10. The top three curves assume the same “large” amplitude of step fluctuations, with different step bunching parameters. From top to bottom: (i) strong bunching, (ii) weak bunching, (iii) no bunching, (iv) fluctuation amplitude reduced by a factor of 5. Note that the top curve corresponds to the disorder realization in (a).

estimates for  $v_v$  and  $F_z(0)$ ,<sup>15</sup> we find that  $A \simeq 18s^2$ , where  $s = 3.9$  nm is the average step separation for a  $2^\circ$  miscut. This result in general agreement with our simulations. For a round plateau, this corresponds to a diameter of about  $5s$ .

The plateau scaling model must break down for very small fields (large  $l_B$ ), when the wave function encloses additional plateaus. At high fields, the scaling also breaks down when the wave function is confined to a single step, saturating at the theoretical upper bound of Ref. 6. For a  $2^\circ$  miscut, this crossover occurs at about 25 T. Thus, the scaling expression in Eq. (4), and possibly the linear experimental data, may correspond to crossover behavior. Finally, we note that the magnetic field dependence of the valley splitting should be first order in the valley coupling parameter  $v_v$ , consistent with Eq. (4), since it involves breaking the positional degeneracy of the mag-

netic (Landau) eigenfunctions.

Valley states can be detrimental for spin-based quantum computing.<sup>21</sup> Large valley splittings are needed to avoid thermal excitations outside the spin-1/2 qubit Hilbert space associated with the valley ground state.<sup>2</sup> To accomplish this in an experimental setting, the present results suggest that we should use substrates without miscuts, although it is usually difficult to eliminate large wavelength roughness in conventional, strained devices. An alternative approach is to develop heterostructures utilizing strain-sharing techniques,<sup>22</sup> which can, in principle, provide step-free interfaces. Indeed, large valley splittings have been obtained in similar unstrained silicon oxide structures.<sup>23</sup>

Finally, we point out that a tilted magnetic field can be used to test the proposed mechanisms for valley splitting suppression. When the magnetic field is tilted away from the growth axis ( $\hat{z}'$ ), we would expect strong variations in the valley splitting, depending on the relative angle of the field with respect to the quantum well.

In summary, we have demonstrated that experimental observations of the magnetic field dependence of the valley splitting are consistent with a theory in which interference between different atomic steps at an interface causes the valley splitting to decrease, as the size of the electronic wave function increases. The present results suggest that valley splitting can be increased by using substrates without miscuts, although it is usually difficult to eliminate large wavelength roughness in conventional, strained devices. Alternatively, valley splitting can be controlled by constraining the wave function with electrostatic gates, as demonstrated in Ref. 24.

### Acknowledgments

The authors would like to acknowledge discussions with S. Chutia, S. Goswami, R. Joynt, G. Klimeck, C. Tahan, and P. von Allmen. This work was supported by NSA and ARDA under ARO Contract No. W911NF-04-1-0389 and by the National Science Foundation through the ITR (DMR-0325634) and EMT (CCF-0523675) programs.

<sup>1</sup> B. E. Kane, Nature (London) **393**, 133 (1998).

<sup>2</sup> M. Friesen, P. Rugheimer, D. E. Savage, M. G. Lagally, D. W. van der Weide, R. Joynt, and M. A. Eriksson, Phys. Rev. B **67**, 121301 (2003).

<sup>3</sup> M. A. Eriksson, M. Friesen, S. N. Coppersmith, R. Joynt, L. J. Klein, K. Slinker, C. Tahan, P. M. Mooney, J. O. Chu, and S. J. Koester, Quant. Inform. Process. **3**, 133 (2004).

<sup>4</sup> C. Herring and E. Vogt, Phys. Rev. **101**, 944 (1956).

<sup>5</sup> T. Ando, A. B. Fowler, and F. Stern, Rev. Mod. Phys. **54**, 437 (1982).

<sup>6</sup> T. B. Boykin, G. Klimeck, M. A. Eriksson, M. Friesen, S. N. Coppersmith, P. von Allmen, F. Oyafuso, and S. Lee,

Appl. Phys. Lett. **84**, 115 (2004); Phys. Rev. B **70**, 165325 (2004).

<sup>7</sup> P. Weitz, R. J. Haug, K. von. Klitzing, and F. Schäffler, Surface Science **361/362**, 542 (1996).

<sup>8</sup> S. J. Koester, K. Ismail, and J. O. Chu, Semicond. Sci. Technol. **12**, 384 (1997).

<sup>9</sup> K. Lai, W. Pan, D. C. Tsui, S. Lyon, M. Mühlberger, and F. Schäffler, Phys. Rev. Lett. **93**, 156805 (2004).

<sup>10</sup> S. Goswami, M. Friesen, J. L. Truitt, C. Tahan, L. J. Klein, J. O. Chu, P. M. Mooney, D. W. van der Weide, S. N. Coppersmith, R. Joynt, and M. A. Eriksson, cond-mat/0408389.

- <sup>11</sup> V. S. Khrapai, A. A. Shashkin, and V. P. Dolgoplov, Phys. Rev. B **67**, 113305 (2003).
- <sup>12</sup> F. J. Ohkawa and Y. Uemura, Journ. Phys. Soc. Japan, **43**, 925 (1977).
- <sup>13</sup> T. Ando, Phys. Rev. B **19**, 3089 (1979).
- <sup>14</sup> W. Kohn, in *Solid State Physics*, edited by F. Seitz and D. Turnbull (Academic Press, New York, 1957), Vol. 5, p. 257.
- <sup>15</sup> M. Friesen, S. Chutia, C. Tahan, S. N. Coppersmith, cond-mat/0608229 (unpublished).
- <sup>16</sup> M. Friesen, Phys. Rev. Lett. **94**, 186403 (2005).
- <sup>17</sup> S. Lee and P. von Allmen, cond-mat/0607462 (unpublished).
- <sup>18</sup> J. H. Davies, *Physics of Low-Dimensional Semiconductors* (Cambridge Press, Cambridge, 1998).
- <sup>19</sup> B. S. Swartzentruber, Y.-W. Mo, R. Kariotis, M. G. Lagally, and M. B. Webb, Phys. Rev. Lett. **65**, 1913 (1990).
- <sup>20</sup> J. Tersoff, Y. H. Phang, Z. Zhang, and M. G. Lagally, Phys. Rev. Lett. **75**, 2730 (1995).
- <sup>21</sup> B. Koiller, X. Hu, and S. das Sarma, Phys. Rev. Lett. **88**, 027903 (2002).
- <sup>22</sup> M. M. Roberts, L. J. Klein, D. E. Savage, K. A. Slinker, M. Friesen, G. Celler, M. A. Eriksson, and M. G. Lagally, Nature Mater. **5**, 388 (2006).
- <sup>23</sup> K. Takashina, Y. Ono, A. Fujiwara, Y. Takahashi, and Y. Hirayama, Phys. Rev. Lett. **96**, 236801 (2006).
- <sup>24</sup> S. Goswami, K. A. Slinker, M. Friesen, L. M. McGuire, J. L. Truitt, C. Tahan, L. J. Klein, J. O. Chu, P. M. Mooney, D. W. van der Weide, R. Joynt, S. N. Coppersmith, and M. A. Eriksson, to appear in Nature Physics.